magnetochemistry

MDPI

Article

New Dmit-Based Organic Magnetic Conductors (PO-CONH-$C_2H_4N(CH_3)_3$)[M(dmit)$_2$]$_2$ (M = Ni, Pd) Including an Organic Cation Derived from a 2,2,5,5-Tetramethyl-3-pyrrolin-1-oxyl (PO) Radical

Hiroki Akutsu [1,*], Scott S. Turner [2] and Yasuhiro Nakazawa [1]

[1] Department of Chemistry, Graduate School of Science, Osaka University, 1-1 Machikaneyama, Toyonaka, Osaka 560-0043, Japan; nakazawa@chem.sci.osaka-u.ac.jp

[2] Department of Chemistry, University of Surrey, Guildford, Surrey GU2 7XH, UK; s.s.turner@surrey.ac.uk

* Correspondence: akutsu@chem.sci.osaka-u.ac.jp; Tel.: +81-6-6850-5399

Academic Editor: Manuel Almeida

Received: 11 January 2017; Accepted: 20 February 2017; Published: 25 February 2017

Abstract: We have prepared two dmit-based salts with a stable organic radical-substituted ammonium cation, (PO-CONH-$C_2H_4N(CH_3)_3$)[Ni(dmit)$_2$]$_2$·CH_3CN and (PO-CONH-$C_2H_4N(CH_3)_3$)[Pd(dmit)$_2$]$_2$ where PO is 2,2,5,5-Tetramethyl-3-pyrrolin-1-oxyl and dmit is 2-Thioxo-1,3-dithiol-4,5-dithiolate. The salts are not isostructural but have similar structural features in the anion and cation packing arrangements. The acceptor layers of both salts consist of tetramers, which gather to form 2D conducting layers. Magnetic susceptibility measurements indicate that the Ni salt is a Mott insulator and the Pd salt is a band insulator, which has been confirmed by band structure calculations. The cationic layers of both salts have a previously unreported polar structure, in which the cation dipoles order as ↗↘↗↘ along the acceptors stacking direction to provide dipole moments. The dipole moments of nearest neighbor cation layers are inverted in both salts, indicating no net dipole moments for the whole crystals. The magnetic network of the [Ni(dmit)$_2$] layer of the Ni salt is two-dimensional so that the magnetic susceptibility would be expected to obey the 1D or 2D Heisenberg model that has a broad maximum around $T \approx \theta$. However, the magnetic susceptibility after subtraction of the contribution from the PO radical has no broad maximum. Instead, it shows Curie–Weiss behavior with C = 0.378 emu·K/mol and $\theta = -35.8$ K. The magnetic susceptibility of the Pd salt obeys a Curie–Weiss model with C = 0.329 emu·K·mol^{-1} and $\theta = -0.88$ K.

Keywords: 1D Heisenberg chains; dmit; organic stable radicals

1. Introduction

Over the past two decades, organic magnetic conductors that combine electrical conductivity with magnetic moments have attracted great interest [1–3]. This is due to reports of unique and interesting properties that emerge from the interplay between itinerant and localized electrons. In particular, λ-(BETS)$_2$FeCl$_4$ (BETS = bis(ethylenedithio)tetraselenafulvalene) and its derivatives show unique physical properties such as a transition to antiferromagnetic order coupled to a metal-insulator transition, colossal magnetoresistance, field-induced superconductivity and a superconductor-to-insulator transition [1]. In fact, many inorganic magnetic anions have already been used as counteranions in organic conductors [2]. Alternatively, researchers have introduced organic free radicals as the source of magnetism [4]. However, thus far, no salts have shown significant magnetic interactions between the conducting electrons and the magnetic moments on the incorporated radicals apart from Sugawara's radical-substituted TTF-based salts [5,6] (TTF = tetrathiafulvalene).

Over the past 15 years, we have prepared several purely organic magnetic conductors, which consist of cationic organic donors (e.g., TTF, bis(ethylenedithio)tetrathiafulvalene (BEDT-TTF)) with monoanionic sulfo ($-SO_3^-$) derivatives of organic free radicals (2,2,6,6-tetramethylpiperidin-1-oxyl (TEMPO) [7–12], 2,2,5,5-tetramethylpyrrolidin-1-oxyl (PROXYL) [13] or 2,2,5,5-Tetramethyl-3-pyrrolin-1-oxyl (PO) [14–18]). Of the salt that we have obtained, none showed a significant interplay between the conducting and localized electrons. This was despite some having evidence of short contacts between the moieties with conducting and those with localized electrons, through short S(BEDT-TTF)···O(Spin centers of the free radicals) distances.

Recently, we have noted that some of these salts have unique structural features, which we have classified into two types, I and II (see Figure 1). Almost all donor-anion type salts consist of 1D or 2D conducting layers interleaved by insulating counterions and/or incorporated neutral molecules. Type I and II salts have structurally unusual anionic layers, in which each individual anisotropic anion aligns in the same orientation as the other anions in the same layer. The result is that each layer has a dipole moment. In Type I salts, such as κ-β″-(BEDT-TTF)$_2$**A1** [15], (TTF)$_3$(**A2**)$_2$ [16] and α′-α′-(BEDT-TTF)$_2$**A3**·H_2O [18] (see Scheme 1 for molecular structures), as illustrated in Figure 1a, the dipole moments of successive anionic layers oppose each other, so there is no net dipole moment. As a consequence, Type I salts have two crystallographically independent cation layers (A and B), one of which (A in Figure 1a) is surrounded by the negative ends of the anionic layer's dipole and the other (B) is bordered by the positive ends of the dipole moments. We also observed self-doping in the Type I salts, where the A layers were more positively charged than B layers. By contrast, a Type II salt, exemplified by α-(BEDT-TTF)$_2$**A4**·3H_2O [17], has a net dipole moment for the whole crystal because all polarized anionic layers are oriented in almost the same direction as shown in Figure 1b. The donor layers of Type II salts also have a dipole moment, which cancels that of the anionic layers. At present, we do not understand the reason why these specific salts possess polarized anionic layers, although it is noted that Type I and II salts all contain sulfo derivatives of the PO radical.

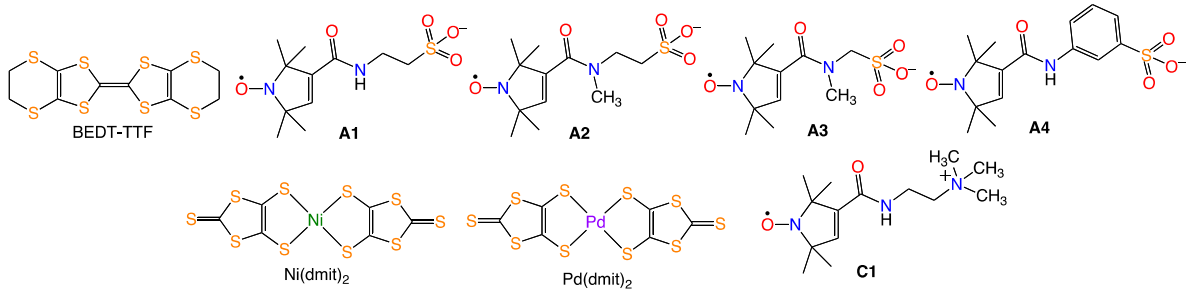

Scheme 1. Molecular structures where the prefixes **A** and **C** stand for anion and cations, respectively.

There are many types of organic conductors, although salts with a conducting donor and counter-anion are the most widely researched, and it is clear that this type has the greatest number of examples of metals and superconductors. This is the reason why we previously concentrated on the synthesis of this type of purely organic magnetic conductors. The second most widely researched type of salt is that with a conducting acceptor and counter-cation, often made with acceptors [M(dmit)$_2$] (where M = Ni, Pd, Pt, etc.). This type has also provided many metals and superconductors [19–21]. Here, we report organic magnetic conductors consisting of [M(dmit)$_2$] (M = Ni and Pd) and a new organic cation bearing PO radical, PO–CONH–$C_2H_4N(CH_3)_3^+$ (**C1**$^+$), the molecular shape of which is similar to that of **A1**. The resultant salts have a new type of structural feature, Type III as shown in Figure 1c.

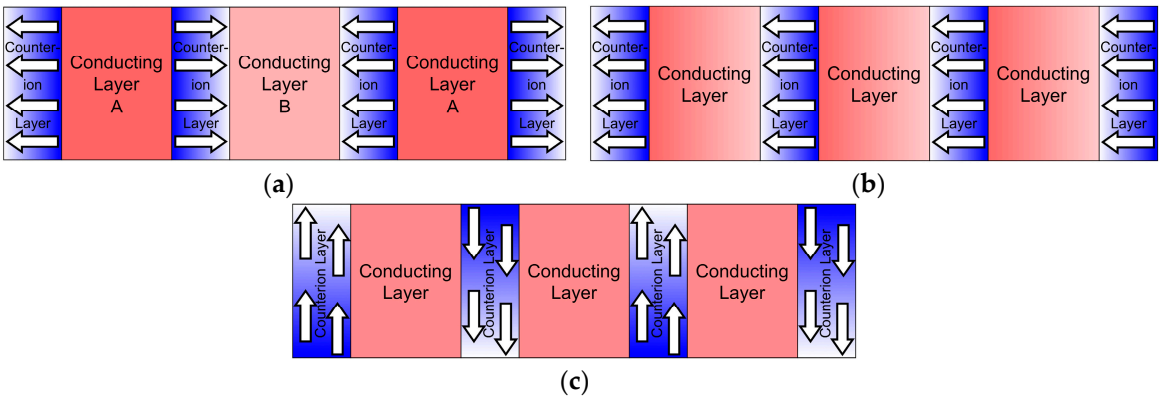

Figure 1. Schematic diagrams of the crystal structures of (**a**) Type I; (**b**) II and (**c**) III salts where the electrical dipoles of the counterions are indicated by arrows, conducting layers are shown as red squares and counterion layers are shown as blue rectangles.

2. Results and Discussion

*2.1. (PO-CONH-$C_2H_4N(CH_3)_3$)Cl (**C1**Cl, **1**)*

Yellow prisms of **1** are deliquescent on exposure to the air so a crystal, suitable for X-ray analysis, was sealed in a capillary tube. X-ray data was collected at 200 K. Figure 2 shows the crystal structure of **1** and indicates the short O···O contact between spin centres. The contacts are approximately 0.8 Å longer than the van der Waals distance (3.04 Å), indicating that the interaction between radicals is weak. Temperature-dependent magnetic susceptibility of a powdered sample of **1** obeys the Curie law with C = 0.377 emu·K·mol^{-1} and θ = −2.1 K.

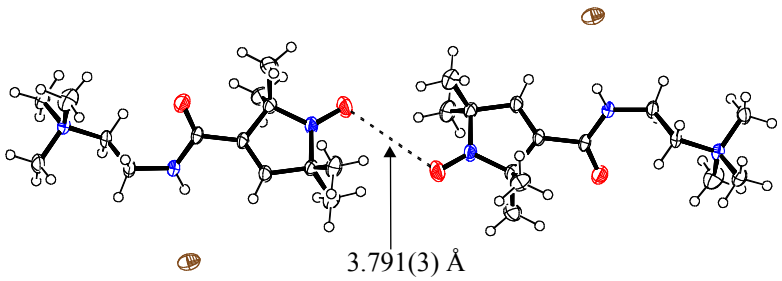

Figure 2. Crystal structure of (PO-CONH-$C_2H_4N(CH_3)_3$)Cl (**1**).

*2.2. (PO-CONH-$C_2H_4N(CH_3)_3$)[Ni(dmit)$_2$]$_2$·CH_3CN ((**C1**)[Ni(dmit)$_2$]$_2$·CH_3CN, **2**)*

The asymmetric unit consists of two [Ni(dmit)$_2$] molecules, a **C1** cation and an incorporated acetonitrile molecule. Figure 3a shows the crystal structure of **2**. The structure has alternating acceptor and cation/acetonitrile layers propagating along the *b*-axis. The structure of the two-dimensional conducting acceptor layer is shown in Figure 3b. Dotted lines indicate short S···S contacts (<3.70 Å). A greater number of short contacts are observed between A–A′ and A–B than between B–B′ along the stacking direction (// *c*), suggesting the formation of B′–A′–A–B tetramers (see also Figure 3c). To confirm tetramer formation, the transfer integrals were calculated using Prof. Takehiko Mori's tight-binding band structure calculation program [22]. The values of *p*1 (A–B), *p*2 (A–A′) and *p*3 (B–B′) (see Figure 3b) are 3.00, 0.87 and -4.54×10^{-3} eV, respectively. The B–B′ interaction, which has fewer short S···S contacts, is approximately five times stronger than that of A–A′, suggesting the formation of a tetramer designated by the A–B–B′–A′. The formula charge of [Ni(dmit)$_2$] is −0.5 so that the charge of the tetramer is −2. This suggests that the salt is either a Mott insulator for which the tetramer would have two spins or a band insulator for which the tetramer consists of spin dimers. The band structure

calculation [22] of **2** has been performed. Figure 4 shows the band dispersions (left) and Fermi surfaces (right) of **2**. There is a mid-gap between the upper and lower bands, which is the so-called "Mott gap", suggesting that the salt is a Mott insulator. Temperature-dependent electrical resistivity of **2** indicates that the salt is a semiconductor with ρ_{RT} = 3.4 Ω·cm and E_a = 0.032 eV. We will further discuss whether the salt is a Mott or band insulator below.

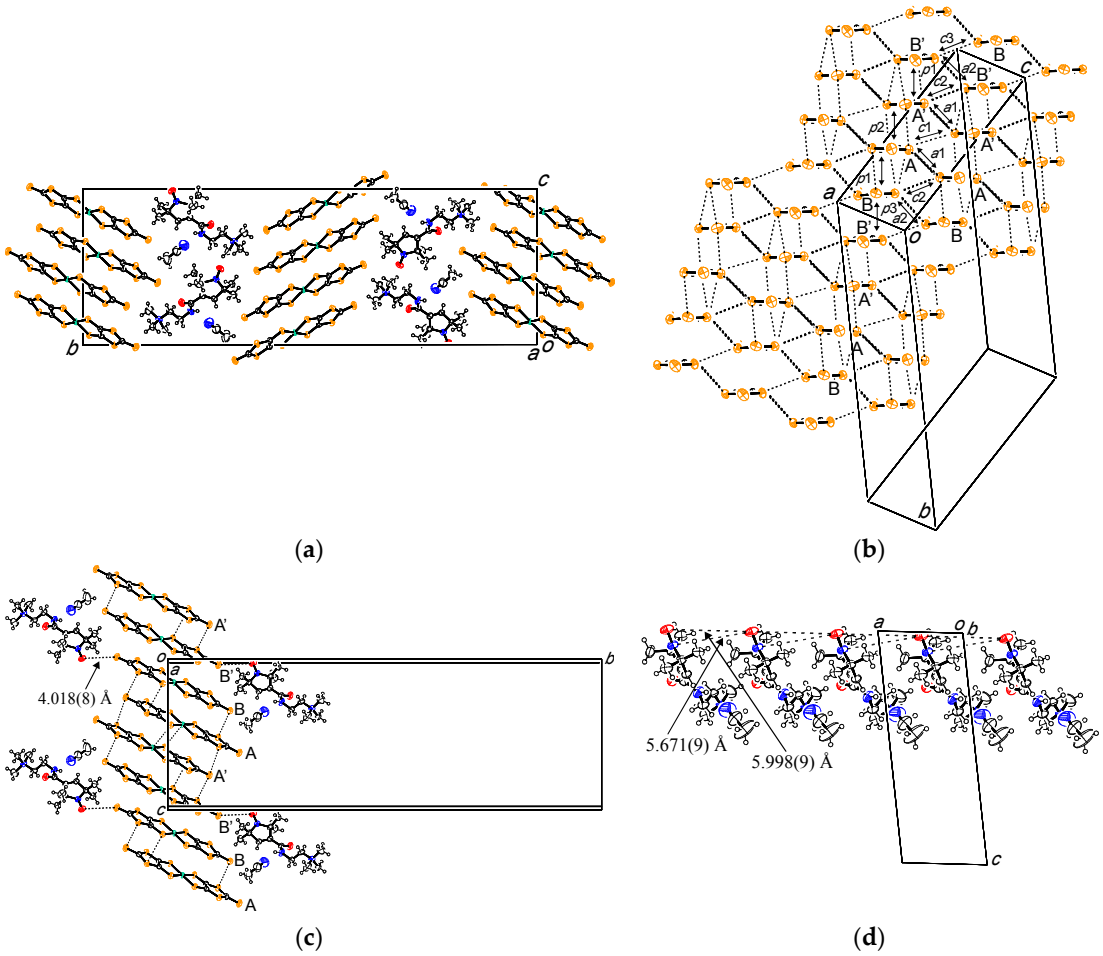

Figure 3. (**a**) crystal structure of **2**; (**b**) [Ni(dmit)$_2$] arrangement in conducting layers of **2**, where dotted lines indicate shorter S···S contacts than the van der Walls distance (3.70 Å); (**c**) interactions between [Ni(dmit)$_2$] and **C1** in **2**, where dotted lines indicate short S···S, S···O and Ni···S (<3.48 Å) contacts and (**d**) 1D magnetic chain of **C1** in (**C1**)[Ni(dmit)$_2$]$_2$·CH_3CN (**2**).

The salt **2** also exhibits magnetically important interactions. Each **C1** cation stacks along the *a*-axis with short contacts between spin centres (N···O and O···O) to form a 1D magnetic chain as shown in Figure 3d. The contacts have longer distances than the van der Waals contacts, but contacts shorter than 6 Å can be significant for magnetic interactions. The spin center O atoms are also close to the outer S atoms of the [Ni(dmit)$_2$] network that forms a 2D conducting sheet as shown in Figure 3c. Thus, the 1D chains of the PO radicals and the 2D layers of the [Ni(dmit)$_2$] molecules interact to form a 2D magnetic system. Magnetic susceptibility measurements of **2** are shown in Figure 5a as a χT-T plot. The right vertical axis indicates $S = 1/2$ spin concentration. The figure indicates that there are approximately two spins at room temperature, suggesting that both the PO radicals of **C1** and also a [Ni(dmit)$_2$]$_2^-$ dimer have one spin. This clearly indicates that the salt **2** is a Mott insulator. The χT value decreases with decreasing temperature, indicating that, at very low temperatures, the magnetic contribution of the [Ni(dmit)$_2$]$_2^-$ dimers is negligible and that of the PO radicals is dominant. We can estimate the contribution of the PO radicals ($\chi_{radical}$) by fitting to a Curie–Weiss expression in the

very low temperature region (2–4 K), yielding C = 0.313 emu·K·mol^{-1} and θ = +0.08 K. The negligibly small Weiss constant suggests that the O···O short contacts between PO radicals (Figure 3d) do not significantly affect the magnetism. To obtain the magnetic contribution of the [Ni(dmit)$_2$] layers, we subtracted the Curie term ($\chi_{radical}$) from the total data (χ_{total}). The resultant $\chi_{[Ni(dmit)_2]}$-T curve is shown in Figure 5b, which can be modeled by the Curie–Weiss law with C = 0.378 emu·K·mol^{-1} and θ = −35.8 K (solid line in Figure 5b). The C value is close to that for S = 1/2 spin (0.375 emu·K·mol^{-1}), suggesting that the $[Ni(dmit)_2]_2^-$ dimer has one spin. The θ value indicates that the spins interact with each other much more strongly than with the spins on **C1**. Organic charge-transfer salts in the Mott insulating state usually have a broad maximums in their χ-T plots at around T = θ as a result of their low dimensionality (1D or 2D Heisenberg systems). However, Figure 5b has no broad maximum and the χ value increases with decreasing temperature. A possible explanation is that **2** may have a 3D magnetic network, although this is not consistent with the structural data from X-ray analysis.

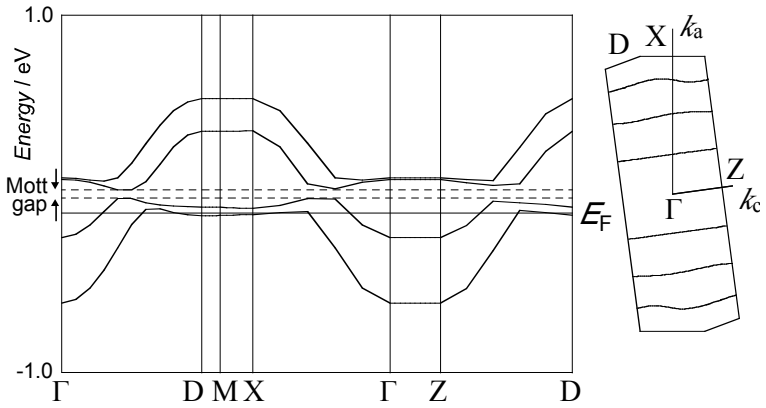

Figure 4. Band dispersions (**left**) and Fermi surfaces (**right**) of **2**. Transfer integrals of $p1$, $p2$, $p3$, $a1$, $a2$, $c1$, $c2$ and $c3$ (see Figure 3b) are 3.00, 0.87, −4.54, −4.14, 21.37, −1.29, −5.94 and −13.89 × 10^{-3} eV, respectively.

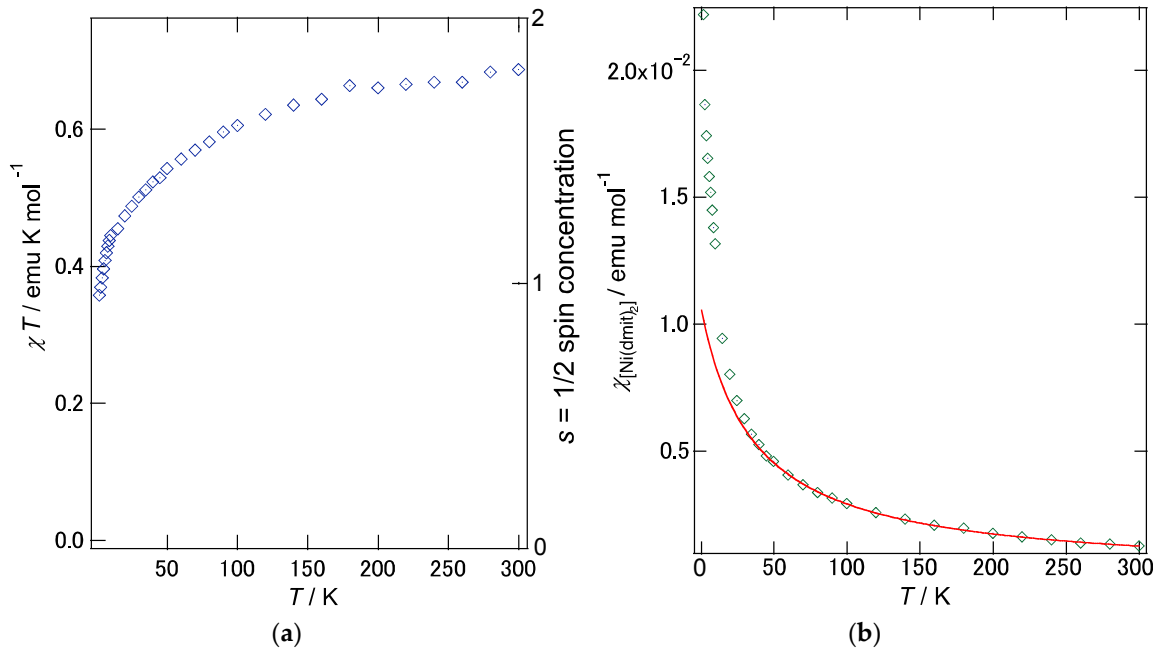

Figure 5. (**a**) χT-T plots of **2**. (**b**) $\chi_{[Ni(dmit)_2]}$-T plots of **2** where $\chi_{[Ni(dmit)_2]} = \chi_{total} - \chi_{radical}$. See text for explanation.

Finally, we discuss the dipole structure of the salt **2**. The salt crystallizes in the monoclinic space group $P2_1/c$, which is centrosymmetric and, therefore, there is no net dipole moment. However, each cation layer has a dipole moment (see Figure 3a). We calculate the dipole moment of **C1** using MOPAC7 [23] to be 23.6 debye. There are two **C1** molecules, which are related by a *c* glide operation, the symmetry operation partially canceling the dipole moments. The dipole moment of the two molecules is calculated by MOPAC7 [23] to be 19.2 debye (D) per one molecule, the direction of the dipole's vector being parallel to the *c*-axis. The dipole moments of nearest neighbor cation layers are crystallographically inverted. Thus, the salt **2** belongs to Type III as shown in Figure 1c.

*2.3. (PO-CONH-$C_2H_4N(CH_3)_3$)[Pd(dmit)$_2$]$_2$ (**(C1)**[Pd(dmit)$_2$]$_2$, **3**)*

Crystals **2** and **3** are not isostructural but they do have similar structural features. The asymmetric unit of **3** contains two [Pd(dmit)$_2$] molecules and a **C1** cation but does not have any incorporated neutral solvent molecules. The structure consists of alternating acceptor and cation layers propagating along the *b*-axis as shown in Figure 6a. Figure 6b shows a conducting layer consisting of [Pd(dmit)$_2$] molecules. The pattern of S···S short contacts indicates that the acceptor layers of compound **3** consist of B–A–A′–B′ tetramers (see also Figure 6a). The transfer integral calculations [22] for $p1$ (A–B) = 44.16, $p2$ (A–A′) = 31.80 and $p3$ (B–B′) = 2.39 $\times$ 10^{-3} eV, which also suggest the formation of a B–A–A′–B′ tetramer. The formula charge of [Pd(dmit)$_2$] is -0.5, indicating a charge per tetramer of -2. This, again, suggests that the salt is a Mott insulator or a band insulator. The ratio of $p2$ (A–A′)/$p3$ (B–B′) of 13.3 indicates that the tetramer in **3** is more isolated than that of **2**, suggesting the formation of a spin dimer and that the salt is a band insulator. If the salt is a Mott insulator like **2**, the salt would be a paramagnet. Figure 7 shows a variable temperature magnetic susceptibility and, unlike for compound **2**, the data can be fitted well by a Curie–Weiss model with C = 0.329 emu·K·mol^{-1}, θ = -0.88 K and an additional temperature independent term a = 3.1 $\times$ 10^{-5} emu·mol^{-1}. The C value is close to 0.375 emu·K·mol^{-1} for 100% of $S = 1/2$ spin, which suggests that the free radical spins on **C1** dominate the Curie–Weiss term. The a value is much less than 2 $\times$ 10^{-4} emu·mol^{-1}, so that the contribution from conduction electrons is negligible (normally, a would be about 2–6 $\times$ 10^{-4} emu·mol^{-1} if the salt is a Pauli paramagnet). These results suggest that compound **3** is a band insulator.

Although no Ni···Ni short contacts were observed in **2** (all >4 Å), short Pd···Pd intra-tetramer contacts in **3** were observed, but no inter-tetramer Pd···Pd contacts are present (Figure 6a). Therefore, the intra-tetramer interactions in **3** are stronger than those in **2**. Band dispersions (Figure 8 left) and a Brillouin zone (Figure 8 right) of **3** show no Fermi surfaces, which also points towards a band insulator description. The temperature-dependent electrical resistivity of **3** indicates that the salt **3** is a semiconductor with ρ_{RT} = 0.81 Ω·cm and E_a = 0.17 eV. The E_a value of **3** is 5.3 times larger than that of **2**. The **C1** cations in **3** form a 1D magnetic chain (Figure 6c); however, the shortest N···O contact of **3** is slightly shorter than 6 Å, indicating that the magnetic interactions are weak. This is consistent with the fact that salt **3** shows a small θ value. Three short S···O contacts between **C1** and [Pd(dmit)$_2$] were observed as shown in Figure 6a. This indicates that the 2D [Pd(dmit)$_2$] layers are connected by a PO radical to form a 3D magnetic network. However, the S···O contacts, ranging from 5.647 to 5.874 Å (Figure 6a) are much longer than those in compound **2** (4.018(8) Å), suggesting that the magnetic interactions within **3** are much weaker than those of **2**, which is again consistent with a small θ value of **3**.

The dipole moment of **C1** in the salt **3** was calculated using MOPAC7 [23]. The value of 22.3 D is slightly smaller than that of **2**. Two **C1** molecules in the unit cell are related by *n* glide operation, which partially cancels their dipole moments. The dipole moment of two molecules is 13.6 D per one molecule, the vector of which is parallel to the *n* (=$a + c$) axis. In addition, [Pd(dmit)$_2$] stacks along the *n*-axis. The dipole moments of nearest neighbor cation layers are opposite. Thus, salt **3** has a structural feature of Type III as shown in Figure 1c.

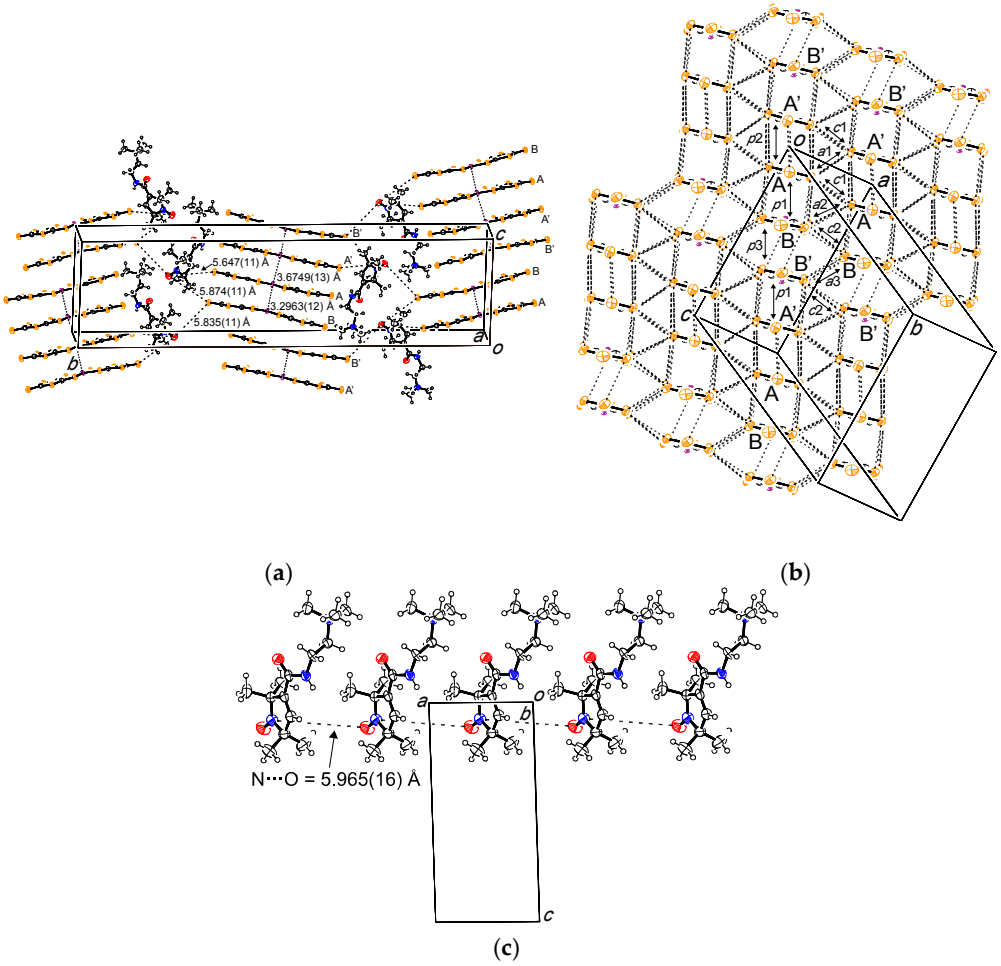

Figure 6. (**a**) crystal structure of **3** where dotted lines indicate the Pd···Pd and S···O short contacts; (**b**) the molecular arrangement in a $[Pd(dmit)_2]$ conducting layer of **3** where dotted lines indicate the short S···S distances (<3.70 Å) and (**c**) the 1D magnetic chain of **C1** in (**C1**)$[Pd(dmit)_2]_2$ (**3**).

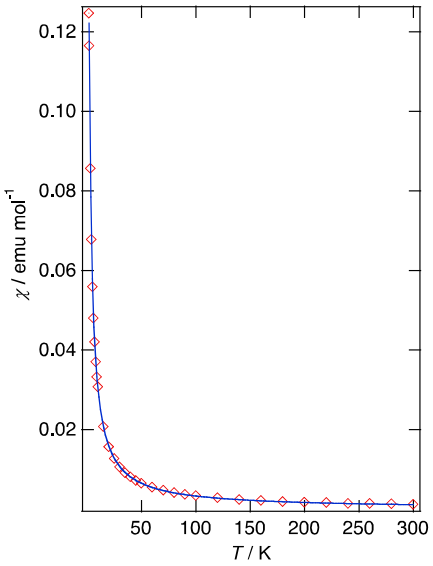

Figure 7. Temperature dependence of the magnetic susceptibility of **3**. The solid line is calculated on the basis of a Curie–Weiss model.

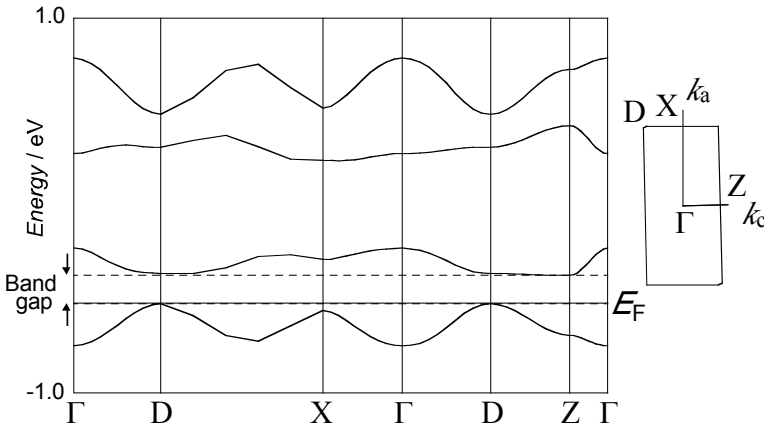

Figure 8. Band dispersions (**left**) and a Brillouin zone (**right**) of **3**. Transfer integrals of *p*1, *p*2, *p*3, *a*1, *a*2, *a*3, *c*1 and *c*2 (see Figure 6b) are 44.16, 31.80, 2.39, 9.47, 4.63, 8.41, −0.60 and -1.61×10^{-3} eV, respectively.

3. Materials and Methods

3-carboxy-2,2,5,5-tetramethyl-3pyrrolin-1-oxyl (PO-COOH) was prepared according to the literature method [24]. **C1**Cl (**1**) was prepared by reacting PO-COOH (1.0 g, 5.4 mmol) with $H_2NC_2H_4N(CH_3)_3Cl{\cdot}HCl$ (0.95 g, 5.4 mmol) in the presence of *N*,*N*′-dicyclohexylcarbodiimide (DCC, 2.7 g, 13 mmol) and 4-dimethylaminopyridine (DMAP, 2.4 g, 20 mmol) in 50 mL of CH_2Cl_2 at room temperature with stirring for two weeks. The resultant solution was filtered, and the filtrate was purified by column chromatography (silica gel, eluents: CH_2Cl_2 then acetone and finally with acetone/methanol = 1:1). Recrystallisation from acetonitrile and ethyl acetate gave hygroscopic yellow rods of **1** (yield 0.63 g (38%); m.p. 209–210 °C). Elemental analysis data were consistent with (**C1**)Cl·0.6H_2O probably because of its strong hygroscopic nature (Anal. Calcd. for $C_{14}H_{27}N_3O_2Cl{\cdot}0.6H_2O$: C, 53.27; H, 9.00; N, 13.31. Found: C, 53.31; H, 8.84; N, 13.30). Constant-current (0.5 μA) electrocrystallisation of **1** (10 mg) with (*n*-$(C_4H_9)_4P$)[Ni(dmit)$_2$] (purchased from Tokyo Chemical Industry Co., Ltd., Tokyo,. Japan (TCI), 10 mg) in acetonitrile (20 mL) in a conventional H-shaped cell yielded black needles of **C1**[Ni(dmit)$_2$]$_2$·CH_3CN (**2**; m.p. >300 °C; Anal. Calcd. for $C_{28}H_{30}N_4O_2S_{20}Ni_2$: C, 27.72; H, 2.49; N, 4.62. Found: C, 27.98; H, 2.50; N, 4.43). Constant-current (1.0 μA) electrocrystallisation of **1** (10 mg) with (*n*-$(C_4H_9)_4N)_2$[Pd(dmit)$_2$] (purchased from TCI, 10 mg) in acetonitrile (20 mL) in a conventional H-shaped cell provided a thin black elongated plates of **C1**[Pd(dmit)$_2$]$_2$ (**3**; m.p. > 300 °C; Anal. Calcd. for $C_{26}H_{27}N_3O_2S_{20}Pd_2$: C, 24.63; H, 2.15; N, 3.31. Found: C, 24.50; H, 2.15; N, 3.09).

X-ray diffraction data of **1**, **2** and **3** were collected at 200, 290 and 250 K, respectively, with a Rigaku Rapid II imaging plate system (Rigaku, Tokyo, Japan) with MicroMax-007 HF/VariMax rotating-anode X-ray generator with confocal monochromated Mo*Kα* radiation. The crystallographic data of **1**, **2** and **3** are listed in Table 1. Electrical resistance measurements were performed by the conventional four-probe method. Temperature dependence of magnetic susceptibility of a polycrystalline sample from 2–300 K was measured using a Quantum Design MPMS-2S SQUID magnetometer (Quantum Design, San Diego, CA, USA). The magnetic susceptibility data of **2** and **3** were corrected for a contribution from an aluminum foil sample folder and the diamagnetic contributions of the samples were estimated from Pascal's constant.

Table 1. Crystallographic data of **1**, **2** and **3**.

Compound	**1**	**2**	**3**
Composition	**C1**Cl	(**C1**)[Ni(dmit)$_2$]$_2$·CH$_3$CN	(**C1**)[Pd(dmit)$_2$]$_2$
Formula	$C_{14}H_{27}N_3O_2Cl_1$	$C_{28}H_{30}O_2N_4S_{20}Ni_2$	$C_{26}H_{27}O_2N_3S_{20}Pd_2$
Fw	304.84	1213.17	1267.52
Space Group	$P2_1/n$	$P2_1/c$	$P2_1/n$
a (Å)	6.2618(3)	5.9977(3)	6.4052(3)
b (Å)	11.5017(7)	47.6504(19)	50.0326(18)
c (Å)	23.6111(14)	16.4464(7)	13.5041(5)
β (°)	92.693(7)	97.507(7)	91.407(6)
V (Å^3)	1698.62(16)	4660.0(4)	4326.3(3)
Z	4	4	4
T (K)	200	290	250
d_{calc} (g·cm^{-1})	1.192	1.729	1.946
μ (cm^{-1})	2.304	17.392	18.309
F (000)	660	2472	2528
2θ range (°)	6–55	6–55	6–55
Total ref.	15621	43525	39491
Unique ref.	3844	10638	9854
R_{int}	0.0337	0.0605	0.0607
Parameters	188	505	478
R_1 ($I > 2\sigma(I)$)	0.066	0.071	0.079
wR_2 (all data)	0.178	0.227	0.217
S	0.981	0.915	1.115
$\Delta\rho_{max}$ (e Å^{-3})	0.61	0.81	1.71
$\Delta\rho_{min}$ (e Å^{-3})	−0.32	−0.71	−1.30
CCDC reference	1532085	1532069	1532070

Each dipole moment of **C1** was calculated using MOPAC7 [23]. The molecular geometry of **C1** was observed in the structure of the relevant charge transfer salt (**2** or **3**) and was used without further structural optimization. In addition, we considered the effect of the incorporated acetonitrile molecule for **2**, which itself has a 3.4 D dipole moment. We performed the dipole moment calculation of one **C1** molecule with the one incorporated CH_3CN molecule by MOPAC7, giving a value of 23.1 D. The calculation of two **C1** cations with the two incorporated CH_3CN molecules by MOPAC2016 [25] was also performed, yielding a value of 19.4 D per one **C1** with one CH_3CN. The value is almost the same as for the result without CH_3CN (19.2 D). All MOPAC calculations were performed using MOPAC keywords of PM3, 1SCF and PRECISE.

4. Conclusions

We have prepared new acceptor-cation type organic magnetic conductors containing an aminoxyl radical: (PO–CONH–$C_2H_4N(CH_3)_3$)[Ni(dmit)$_2$]$_2$·CH_3CN (**2**) and (PO–CONH–$C_2H_4N(CH_3)_3$)[Pd(dmit)$_2$]$_2$ (**3**). Neither salt shows significant magnetic interactions between itinerant and localized electrons. An interesting feature is that they have similar structural features, in that they do not have net dipole moments but possess a periodicity of dipoles that we have termed Type III structures. The magnetic susceptibility measurements and band structure calculations indicate that **2** is a Mott insulator and **3** is a band insulator.

Acknowledgments: The authors thank Shusaku Imajo at Osaka Unversity for help with electrical resistivity measurements. This work was supported by the Murata Science Foundation, Nagaokakyo, Japan.

Author Contributions: H.A. conceived and designed the experiments. H.A. performed the experimental work. All authors contributed to the preparation of the manuscript.

Conflicts of Interest: The authors declare no conflict of interest.

References

1. Kobayashi, H.; Cui, H.; Kobayashi, A. Organic metals and superconductors based on BETS (BETS = bis(ethylenedithio)tetraselenafulvalene. *Chem. Rev.* **2004**, *104*, 5265–5288. [CrossRef] [PubMed]
2. Day, P.; Coronado, E. Magnetic molecular conductors. *Chem. Rev.* **2004**, *104*, 5419–5448.
3. Vyaselev, O.M.; Kartsovnik, M.V.; Biberacher, W.; Zorina, L.V.; Kushch, N.D.; Yagubskii, E.B. Magnetic transformations in the organic conductor κ-$(BETS)_2Mn[N(CN)_2]_3[N(CN)_2]_3$ at the metal-insulator transition. *Phys. Rev. B* **2011**, *83*, 094425:1–094425:6. [CrossRef]
4. Nakatsuji, S. Preparations, Reactions, and Properties of Functional Nitroxide Radicals. In *Nitroxide: Application in Chemistry, Biomedicine, and Materials Chemistry*; Likhtenshtein, G.I., Yamauchi, J., Nakatsuji, S., Smirnov, A.I., Tamura, R., Eds.; Wiley-VCH: Weinheim, Germany, 2008; pp. 161–204.
5. Matsushita, M.M.; Kawakami, H.; Kawada, Y.; Sugawara, T. Negative Magneto-resistance Observed on an Ion-radical Salt of a TTF-based Spin-polarized Donor. *Chem. Lett.* **2007**, *36*, 110–111. [CrossRef]
6. Sugawara, T.; Komatsu, H.; Suzuki, K. Interplay between magnetism and conductivity derived from spin-polarized donor radicals. *Chem. Soc. Rev.* **2011**, *40*, 3105–3118. [CrossRef] [PubMed]
7. Akutsu, H.; Yamada, J.; Nakatsuji, S. Preparation and characterization of novel organic radical anions for organic conductors: TEMPO–$NHSO_3^-$ and TEMPO-OSO_3^-. *Synth. Met.* **2001**, *120*, 871–872. [CrossRef]
8. Akutsu, H.; Yamada, J.; Nakatsuji, S. A New Organic Anion Consisting of the TEMPO Radical for Organic Charge-Transfer Salts: 2,2,6,6-Tetramethylpiperidinyloxy-4-sulfamate (TEMPO–$NHSO_3^-$). *Chem. Lett.* **2001**, *30*, 208–209. [CrossRef]
9. Akutsu, H.; Yamada, J.; Nakatsuji, S. New BEDT-TTF-based Organic Conductor Including an Organic Anion Derived from the TEMPO Radical, α-$(BEDT\text{-}TTF)_3(TEMPO\text{–}NHCOCH_2SO_3)_2\cdot 6H_2O$. *Chem. Lett.* **2003**, *32*, 1118–1119. [CrossRef]
10. Akutsu, H.; Masaki, K.; Mori, K.; Yamada, J.; Nakatsuji, S. New organic free radical anions TEMPO-*A*-CO-(*o*-, *m*-, *p*-)$C_6H_4SO_3^-$ (*A* = NH, NCH_3, O) and their TTF and/or BEDT-TTF salts. *Polyhedron* **2005**, *24*, 2126–2132. [CrossRef]
11. Yamashita, A.; Akutsu, H.; Yamada, J.; Nakatsuji, S. New organic magnetic anions TEMPO–CONA$(CH_2)_nSO_3^-$ (*n* = 0–3 for *A* = H, *n* = 2 for *A* = CH_3) and their TTF, TMTSF and/or BEDT-TTF salts. *Polyhedron* **2005**, *16*, 2796–2802. [CrossRef]
12. Akutsu, H.; Yamada, J.; Nakatsuji, S.; Turner, S.S. A novel BEDT-TTF-based purely organic magnetic conductor, α-$(BEDT\text{-}TTF)_2(TEMPO\text{–}N(CH_3)COCH_2SO_3)\cdot 3H_2O$. *Solid State Commun.* **2006**, *140*, 256–260. [CrossRef]
13. Akutsu, H.; Sato, K.; Yamashita, S.; Yamada, J.; Nakatsuji, S.; Turner, S.S. The first organic paramagnetic metal containing the aminoxyl radical. *J. Mater. Chem.* **2008**, *18*, 3313–3315. [CrossRef]
14. Akutsu, H.; Yamashita, S.; Yamada, J.; Nakatsuji, S.; Turner, S.S. Novel Purely Organic Conductor with an Aminoxyl Radical, α-$(BEDT\text{-}TTF)_2(PO\text{–}CONHCH_2SO_3)\cdot 2H_2O$ (PO = 2,2,5,5-Tetramethyl-3-pyrrolin-1-oxyl Free Radical). *Chem. Lett.* **2008**, *37*, 882–883. [CrossRef]
15. Akutsu, H.; Yamashita, S.; Yamada, J.; Nakatsuji, S.; Hosokoshi, Y.; Turner, S.S. A Purely Organic Paramagnetic Metal, κ-β″-$(BEDT\text{-}TTF)_2(PO\text{–}CONHC_2H_4SO_3)$, Where PO = 2,2,5,5-Tetramethyl-3-pyrrolin-1-oxyl Free Radical. *Chem. Mater.* **2011**, *23*, 762–764. [CrossRef]
16. Akutsu, H.; Kawamura, A.; Yamada, J.; Nakatsuji, S.; Turner, S.S. Anion polarity-induced dual oxidation states in a dual-layered purely organic paramagnetic charge-transfer salt, $(TTF)_3(PO\text{–}CON(CH_3)C_2H_4SO_3)_2$, where PO = 2,2,5,5-tetramethyl-3-pyrrolin-1-oxyl free radical. *CrystEngComm* **2011**, *13*, 5281–5284. [CrossRef]
17. Akutsu, H.; Ishihara, K.; Yamada, J.; Nakatsuji, S.; Turner, S.S.; Nakazawa, Y. A strongly polarized organic conductor. *CrystEngComm* **2016**, *18*, 8151–8154. [CrossRef]
18. Akutsu, H.; Ishihara, K.; Ito, S.; Nishiyama, F.; Yamada, J.; Nakatsuji, S.; Turner, S.S.; Nakazawa, Y. Anion Polarity-Induced Self-doping in Purely Organic Paramagnetic Conductor, α′-α′-$(BEDT\text{-}TTF)_2$ (PO-CONH-*m*-$C_6H_4SO_3)\cdot H_2O$ where BEDT-TTF is Bis(ethylenedithio)tetrathiafulvalene and PO is 2,2,5,5-Tetramethyl-3-pyrrolin-1-oxyl Free Radical. *Polyhedron* **2017**, in press. [CrossRef]
19. Kato, R. Conducting Metal Dithiolene Complexes: Structural and Electronic Properties. *Chem. Rev.* **2004**, *104*, 5319–5346. [CrossRef] [PubMed]
20. Kobayashi, H.; Kobayashi, A.; Tajima, H. Studies on Molecular Conductors: From Organic Semiconductors to Molecular Metals and Superconductors. *Chem. Asian J.* **2011**, *6*, 1688–1704. [CrossRef] [PubMed]

21. Cassoux, P.; Valade, L.; Kobayashi, H.; Kobayashi, A.; Clark, R.A.; Underhill, A.E. Molecular metals and superconductors derived from metal complexes of 1,3-dithiol-2-thione-4,5-dithiolate (dmit). *Coord. Chem. Rev.* **1991**, *110*, 115–160. [CrossRef]
22. Mori, T.; Kobayashi, A.; Sasaki, Y.; Kobayashi, H.; Saito, G.; Inokuchi, H. The Intermolecular Interaction of Tetrathiafulvalene and Bis(ethylenedithio)tetrathiafulvalene in Organic Metals. Calculation of Orbital Overlaps and Models of Energy-band Structures. *Bull. Chem. Soc. Jpn.* **1984**, *57*, 627–633. [CrossRef]
23. Stewart, J.J.P. *MOPAC7*, Stewart Computational Chemistry: Colorado Springs, CO, USA, 1993.
24. Rozantsev, E.G. *Free Nitroxide Radicals*; Plenum Press: New York, NY, USA; London, UK, 1970.
25. Stewart, J.J.P. *MOPAC2016*, Stewart Computational Chemistry: Colorado Springs, CO, USA, 2016.